NANO LETTERS

pubs.acs.org/NanoLett

Letter

Portable Triboelectric Electrostatic Tweezer for External Manipulation of Droplets within a Closed Femtosecond Laser-Treated Superhydrophobic System

Jiale Yong, Xinlei Li, Youdi Hu, Yiming Wang, Yubin Peng, Zhenrui Chen, Yachao Zhang, Suwan Zhu, Chaowei Wang,* and Dong Wu*

Cite This: *Nano Lett.* 2024, 24, 7116−7124

Read Online

ACCESS | Metrics & More | Article Recommendations | Supporting Information

ABSTRACT: Controllable droplet manipulation has diverse applications; however, limited methods exist for externally manipulating droplets in confined spaces. Herein, we propose a portable triboelectric electrostatic tweezer (TET) by integrating electrostatic forces with a superhydrophobic surface that can even manipulate droplets in an enclosed space. Electrostatic induction causes the droplet to be subjected to an electrostatic force in an electrostatic field so that the droplet can be moved freely with the TET on a superhydrophobic platform. Characterized by its high precision, flexibility, and robust binding strength, TET can manipulate droplets under various conditions and achieve a wide range of representative fluid applications such as droplet microreactors, precise self-cleaning, cargo transportation, the targeted delivery of chemicals, liquid sorting, soft droplet robotics, and cell labeling. Specifically, TET demonstrated the ability to manipulate internal droplets from the outside of a closed system, such as performing cell labeling experiments within a sealed Petri dish without opening the culture system.

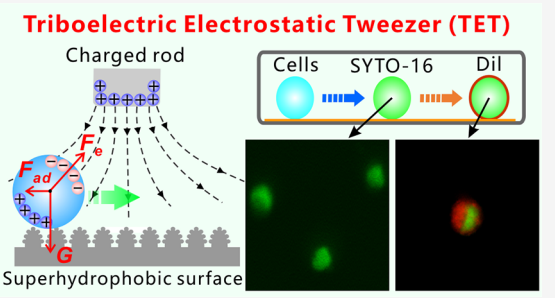

KEYWORDS: *droplet manipulation, superhydrophobic surface, triboelectric electrostatic tweezer, electrostatic force, femtosecond laser*

Downloaded via UNIV SCIENCE AND TECHNOLOGY CHINA on June 17, 2024 at 06:38:20 (UTC).
See https://pubs.acs.org/sharingguidelines for options on how to legitimately share published articles.

Controllable droplet manipulation plays an indispensable role in various applications, such as microfluidics,[1,2] printing technology,[3,4] biological detection and analysis,[5,6] combinatorial chemistry,[7,8] water harvesting,[9,10] and heat management.[11,12] Due to the risk of contamination associated with contact operation, contactless droplet manipulation has attracted increasing attention in recent years. There are usually two strategies for achieving noncontact transport of droplets.[13−15] One is to design geometric, chemical, wetting, or even charge gradient structures on the surface of solid materials.[16−20] The droplets on the gradient structures have asymmetric three-phase contact lines or contact angles, which enable the droplets to move along the gradient direction spontaneously under the asymmetric forces (e.g., Laplace force).[13,14] However, droplet manipulation based on gradient structures is limited by short transport distances, single and fixed transport directions, and irreversible movement, arising from the foundation of these methods (i.e., the limited gradient range and the fixed gradient direction).[19,21] Another idea is to change the morphology or other physical and chemical properties of the substrate supporting the droplet through external stimuli (such as magnetism,[22] light,[23,24] and electricity[25]) or to directly apply force to the droplets,[26−28] making the droplet follow the stimulus source to move forward. Although stimulus strategies allow droplets to move farther and in a more flexible direction than gradient structures, they often rely on essential surface pretreatment or droplet pretreatment.[23,24,29−31] Nonetheless, despite extensive progress, these contactless manipulations are usually carried out on open material surfaces, and few methods are capable of manipulating droplets in a confined space from the outside without surface or droplet pretreatment. External manipulation of droplets in closed spaces is very useful for many practical applications when the system is not allowed to open or conventional tools cannot be inserted into the system; it is still a challenge to achieve such a novel function.

In contrast to the magnetism and light stimuli, which drive droplets indirectly by changing the physical and chemical properties of the operating platform,[22−24] an electrostatic field can directly apply electrostatic force to droplets.[26,27] In addition, the electric field can easily penetrate the insulating material, so electrostatic forces show great potential for droplet manipulation in confined environments. However, electrostatic operating systems based on a high-voltage input are unsafe, not easy to carry, and not convenient enough. There is an urgent

Received: April 24, 2024
Revised: May 30, 2024
Accepted: June 3, 2024
Published: June 4, 2024

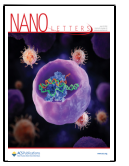

ACS Publications

© 2024 American Chemical Society

https://doi.org/10.1021/acs.nanolett.4c01953
Nano Lett. 2024, 24, 7116−7124

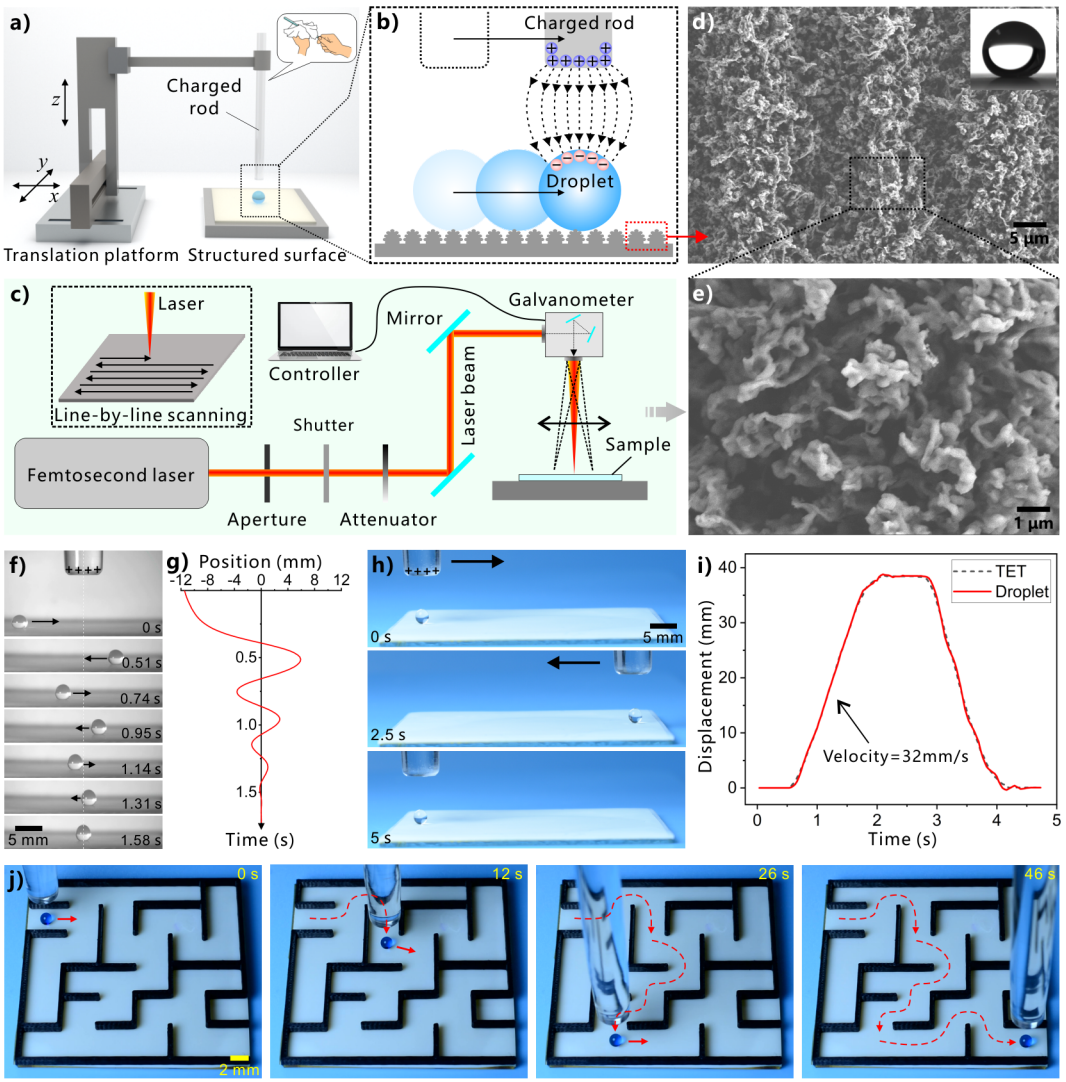

Figure 1. Designed system for droplet manipulation by triboelectric electrostatic tweezers. (a) Schematic of the manipulation system. (b) Schematic of moving a droplet by electrostatic interactions. (c) Femtosecond laser processing system. Inset: line-by-line scanning method. (d, e) Laser-induced superhydrophobic microstructures on the PTFE surface. Inset: a water droplet on this surface. (f) Process of TET clawing back a droplet that deviates from its center. (g) Position change of the droplet in (f). (h) A round-trip process in which the droplet was moved forward and returned. (i) The position changes of the TET and the droplet during droplet manipulation in (h). (j) A droplet being guided through a complex maze.

need to develop a safer and more convenient electrostatic operation method for manipulating droplets under different conditions.

Here, a portable triboelectric electrostatic tweezer (TET) was developed to manipulate droplets not only in open space but also in enclosed space. Electrostatic induction of droplets occurs under the electric field generated by the charged rod; thus, the electrostatic force allows the droplet to move freely on the superhydrophobic platform with the TET. TET droplet manipulation has the characteristics of high precision, high flexibility, and strong binding strength to droplets. These features enable the TET to manipulate droplets under a variety of conditions and to achieve a range of droplet-related applications. In particular, TET can manipulate droplets in a closed plastic tube and enable cell labeling experiments in an enclosed Petri dish without opening the culture system.

Figure 1a shows the designed TET system for droplet manipulation. A glass rod that is positively charged by rubbing silk is vertically fixed to a 3D mobile mechanism. The charged rod is above the droplet on the operating platform and is at a suitable distance from the droplet. To move the droplets easily, the operating platform must have extremely low adhesion to the droplets. A superhydrophobic platform was easily obtained by using a femtosecond laser to ablate the surface of a hydrophobic polytetrafluoroethylene (PTFE) sheet (Figure 1c). Laser processing produces hierarchical microstructures on the PTFE surface (Figure 1d and e). The resultant surfaces are superhydrophobic with a contact angle of 152.6 ± 1.7° (inset of Figure 1d) and a sliding angle of 2.3 ± 0.5° (Figure S1) to water droplets and thus have extremely low adhesion to droplets. The droplets on the superhydrophobic platform are affected by the electric field generated by the electrostatic rod and subjected to electrostatic forces due to electrostatic induction.[32,33] As shown in Figure 1b, the electrostatic force tightly binds the droplet to the location directly below the rod. As the charged rod moves horizontally, the droplets will move with it, as if controlled by an invisible tweezer, i.e., a triboelectric electrostatic tweezer.

Figure 1f and g depict the process by which TET pulls an off-center droplet back. Under electrostatic attraction, the droplet

https://doi.org/10.1021/acs.nanolett.4c01953
Nano Lett. 2024, 24, 7116−7124

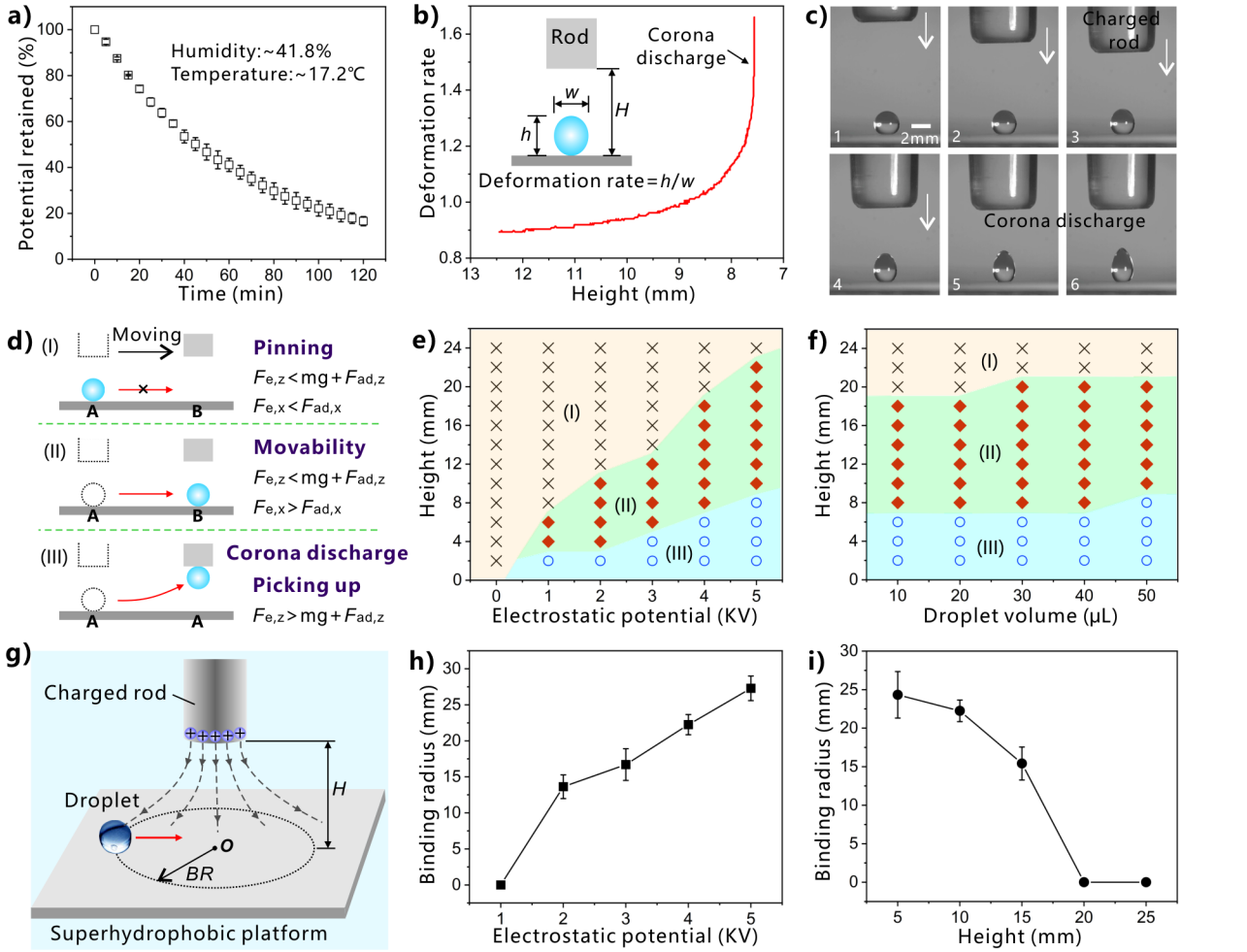

Figure 2. Factors affecting droplet manipulation. (a) Degradation of the electrostatic potential of the charged rod under a humidity of ~41.8% and a temperature of ~17.2 °C. (b) Change in the deformation rate of the droplet as the height of the TET gradually decreases. Inset: definition of the deformation rate. (c) Snapshots of droplet shape with gradually decreasing TET height. (d) Schematic showing three different conditions for electrostatic droplet manipulation. (e) Phase diagram showing the influence of the electrostatic potential and the height of the TET on droplet manipulation. (f) Phase diagram showing the effect of droplet volume on electrostatic droplet manipulation. (g) Schematic and definition of the binding radius. (h, i) Influence of (h) the electrostatic potential (H = 10 mm) and (i) the height (U = +4 kV) of the TET on the binding radius.

quickly moves toward the TET and finally stops below the TET after a damping process (Movie S1). Even if the droplet is moving faster than 80 mm/s, it can be attracted back (Figure S2), indicating the strong binding ability of the TET to droplets. On the superhydrophobic platform, the motion of the droplets can be guided by moving the charged rod. Figure 1h and Movie S2 show a round-trip process in which the droplet is moved forward and returned by TET at an average velocity of ~32 mm/s. The position changes of the TET and droplet indicate that the lag of the droplet is very small (Figure 1i). Even when the velocity increases to ~101.8 mm/s, the droplet is still synchronous with the motion of the TET (Movie S2), showing a very high precision of droplet manipulation. In addition to high precision, the TET also has a strong flexibility for manipulating droplets. Figure 1j and Movie S3 show the process of successfully guiding droplets through a complex maze by TET.

A low air humidity is beneficial for stabilizing the surface charge on the triboelectric rod.[19] Despite the degradation of the surface charge in a normal environment (humidity ≈ 41.8%, temperature ≈ 17.2 °C), we found the electrostatic potential remained at 87.5% after 10 min, which is sufficient to complete the droplet manipulation task (Figure 2a). The droplet under the TET is lengthened vertically into an ellipsoid shape because of electrostatic attraction (Figure 1b and c). The degree of droplet deformation can be described by the deformation rate, h/w, where h is the vertical height and w is the horizontal diameter of the droplet. With decreasing height (H) of the TET, the deformation rate increases, which indicates that the droplet is subjected to a stronger electrostatic attraction (Movie S4). When H is less than a safe value, either a corona discharge process occurs (the droplet is instantly stretched, thus coming into contact with the rod, and the droplet is charged)[33−35] or the droplet leaves the superhydrophobic substrate. The results indicate that the electrostatic force received by the droplet is also related to the distance from the TET, in addition to the surface electrostatic potential of the TET.

The electrostatic potential (U) and H of the TET have crucial influences on the droplet manipulation. As shown in Figure 2d and e, droplet manipulation occurs under three different conditions. When U is too low and H is too large (region I), the electrostatic force (F_e) on the droplets is very small. Its horizontal component ($F_{e,x}$) is not enough to overcome the adhesive force ($F_{ad,x}$) of the platform to the droplet, so the droplet cannot be moved. As the U of the TET increases or H

https://doi.org/10.1021/acs.nanolett.4c01953
Nano Lett. 2024, 24, 7116−7124

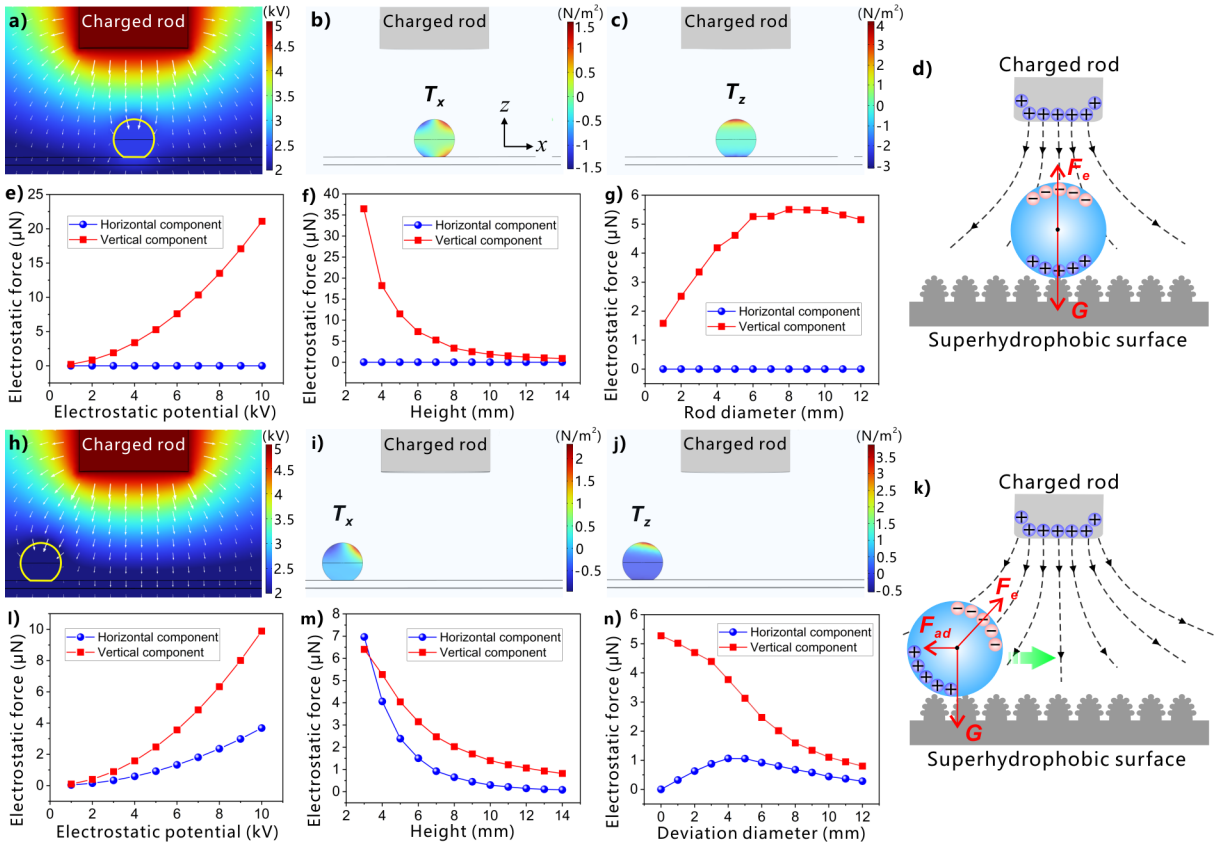

Figure 3. Understanding the mechanism of TET droplet manipulation via simulation and force analysis. (a, h) Distribution of the electrostatic potential and electric field intensity (the arrows reflecting its direction and strength) around a +5 kV charged rod. (b, c, i, j) Distribution of the Maxwell stress tensor applied to a droplet (T_x, horizontal component; T_z, vertical component). (d, k) Force analysis of the droplets under electrostatic interactions. (e−g, l−n) Simulation results of the electrostatic forces acting on a droplet: (e) at different U values (H = 7 mm, D = 7 mm), (f) at different H values (U = +5 kV, D = 7 mm), (g) at different D values (U = +5 kV, H = 7 mm), (l) at different U values (H = 7 mm, D = 7 mm, DD = 6 mm), (m) at different H values (U = +5 kV, D = 7 mm, DD = 6 mm), and (n) at different DD values (U = +5 kV, H = 7 mm, D = 7 mm). (a)−(g) show the conditions when the droplet is directly below the TET (DD = 0 mm), and (h)−(n) show the conditions when the droplet deviates horizontally from the TET by a certain distance (DD ≠ 0 mm).

decreases, the electric field strength at the droplet position increases, and the droplet is attracted by a larger F_e. When $F_{e,x}$ can overcome $F_{ad,x}$, the droplet will move forward, following the TET (region II). However, when the U is too high or the H of the TET is too low, the droplet will be subjected to excessive electrostatic attraction (region III). Once the vertical electrostatic force ($F_{e,z}$) is strong enough to overcome the gravity (mg) of the droplet, the droplet will detach from the superhydrophobic platform and be picked up by the TET, making it impossible to manipulate the droplet. The droplet can be manipulated flexibly only if the TET has a suitable U and is at a suitable H (i.e., a suitable distance from the droplet) (Figure 2e). Figure 2f shows the effect of the droplet volume on electrostatic droplet manipulation. Droplets of different sizes can be moved, and the droplet volume has less influence on the manipulation process than the electrostatic potential and height of the TET.

During droplet manipulation, only droplets within a certain distance of the TET can be pulled back to the position below the TET, and droplets beyond this distance cannot be controlled. This critical range can be characterized by the binding radius (BR) (Figure 2g). As shown in Figure 2h and i, the BR increases with increasing potential of the TET and decreases with increasing height of the TET because a larger electrostatic potential or a smaller height can increase the binding strength of the TET to the droplets.

Figure 3 reveals the mechanism of the TET droplet manipulation. As shown in Figure 3a and h, an electrostatic field is created around the TET. Spatially, the electric potential and the electric field strength gradually decrease as the distance from the charged rod increases. Under the electrostatic field, electrostatic induction redistributes charges inside the droplet and generates induced charges.[32,33,36] Taking the TET with a positive potential as an example, the positive charge inside the droplet accumulates on the droplet surface away from the TET due to the repulsive force. In contrast, the negative charge accumulates on the droplet surface near the TET due to attraction. The uneven distribution of charge causes the droplet to be subjected to electrostatic force (Figure 3d and k). The Coulomb force is the sum of the Maxwell stresses acting on the surface of the droplet:[19,37−39]

$$\boldsymbol{F}_e = \oint \left[\varepsilon \boldsymbol{E}(\boldsymbol{E}\boldsymbol{n}) - \frac{\varepsilon}{2}\boldsymbol{E}^2\boldsymbol{n} \right] \mathrm{d}S \quad (1)$$

where ε and $\boldsymbol{E}$ are the permittivity of the liquid and the electric field strength at the droplet surface, respectively, and $\boldsymbol{n}$ and S are the surface unit normal and surface area of the droplet, respectively. This electrostatic force can be quantified in tensor form:[26,40,41]

https://doi.org/10.1021/acs.nanolett.4c01953
Nano Lett. 2024, 24, 7116−7124

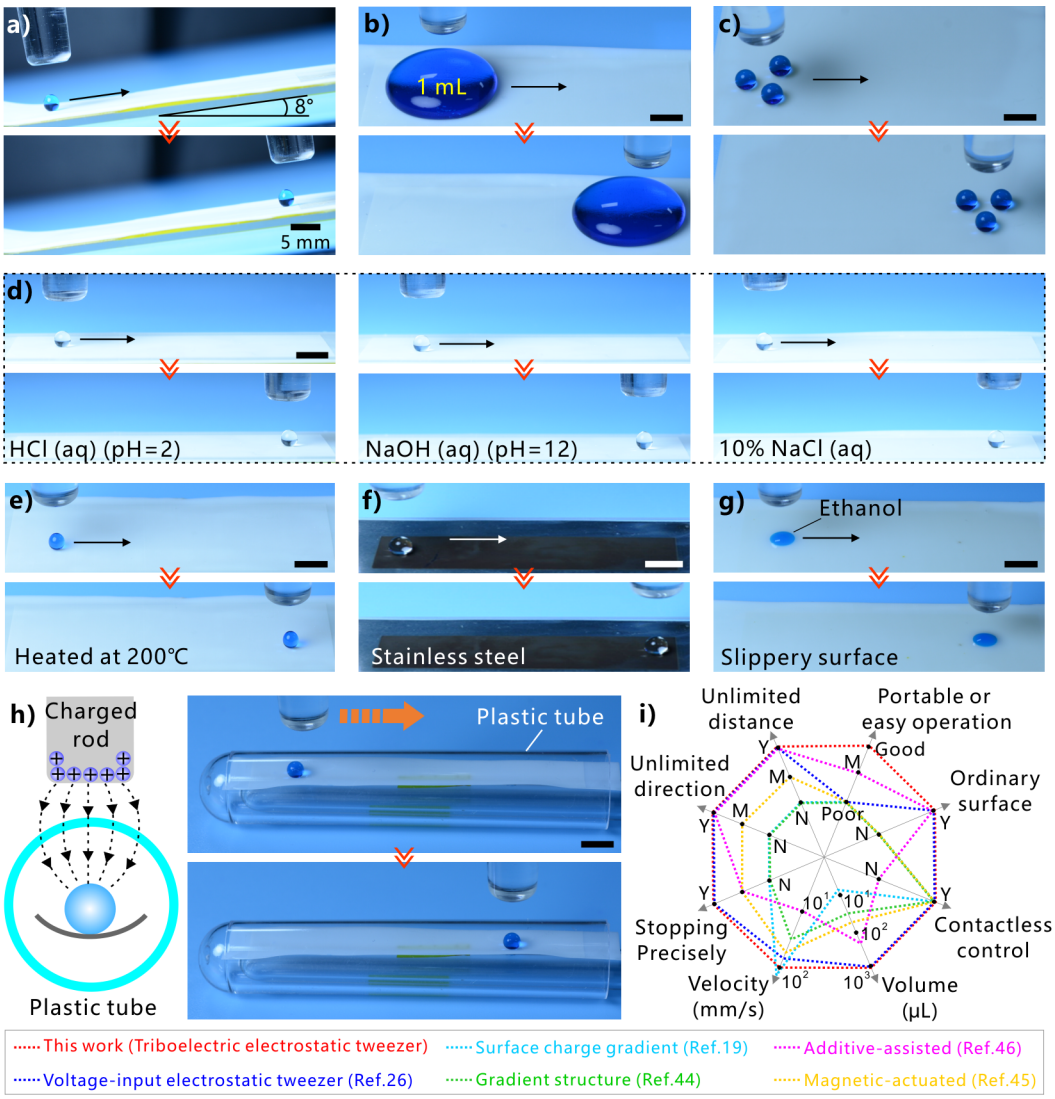

Figure 4. Multifunctional droplet manipulation based on the TET. (a) Driving a droplet to move upward along an inclined surface. (b) Manipulating a large droplet with a volume of 1 mL. (c) Parallel manipulation of multiple droplets by a single TET. (d) Manipulation of various corrosive acid, alkali, and salt solutions. (e) Droplet manipulation on the surface after heating treatment. (f) Manipulation of droplets on an electrically conductive superhydrophobic stainless steel surface. (g) Manipulation of an ethanol droplet with a surface tension of 22.3 mN/m on the lubricated slippery PTFE surface. (h) Manipulating a droplet in an enclosed PS plastic tube from the outside. (i) Comparison between the TET and other reported techniques for droplet manipulation from eight aspects.[19,26,44−46] "Y", "N", and "M" denote yes, no, and medium, respectively. The instructions in the bottom box correspond to (i). Scale bar = 5 mm.

$$\boldsymbol{F}_e = \oint T_{e,ij} \cdot \boldsymbol{n} \mathrm{d}S, \quad \text{with } T_{e,ij} = \varepsilon_0 \left(E_i E_j - \frac{\delta_{ij}}{2} E^2 \right), \; i, j = x, y, z \tag{2}$$

where $\boldsymbol{T}_e$, ε_0, E, and δ_{ij} are the Maxwell stress tensor, the permittivity of air, the magnitude of $\boldsymbol{E}$, and the Kronecker delta function, respectively. The distribution of $\boldsymbol{T}_e$ on the droplet can be calculated via COMSOL-Multiphysics simulation, reflecting the forces acting on different units on the droplet surface, as shown in Figure 3b, c, i, and j.

Since the accumulated negative charge is closer to the TET and the electric field strength at the location of negative charge is greater than that at the positive charge, the attraction of negative charge is greater than the repulsion of positive charge. Overall, the attraction dominates, so that the electrostatic force is directed toward the TET, which provides the driving force for the movement of droplets. When the droplet is directly under the TET, the $F_{e,z}$ is positively correlated with the U (Figure 3e), negatively correlated with the H (Figure 3f), and positively correlated with the diameter (D) of the TET when $D \leq 8$ mm (Figure 3g). However, $F_{e,x}$ is always 0, so the droplet does not move laterally and stays under the TET (Figure 3d). When the droplet deviates horizontally from the TET by a certain distance, both the $F_{e,x}$ and the $F_{e,z}$ have a positive relation with U (Figure 3) and are negatively correlated with H of the TET (Figure 3m). The $F_{e,z}$ decreases as the deviation distance (DD) from the TET gradually increases, while the $F_{e,x}$ first increases and then decreases (Figure 3n). Figure 3k shows the force analysis of the droplet when it deviates from the TET. The droplet is subjected to the electrostatic Coulomb force (F_e), gravity (G), and adhesive force (F_{ad}). When only the horizontal motion of the droplets is considered, the driving force is

$$F = F_e \cos \beta - F_{ad} \tag{3}$$

https://doi.org/10.1021/acs.nanolett.4c01953
Nano Lett. 2024, 24, 7116−7124

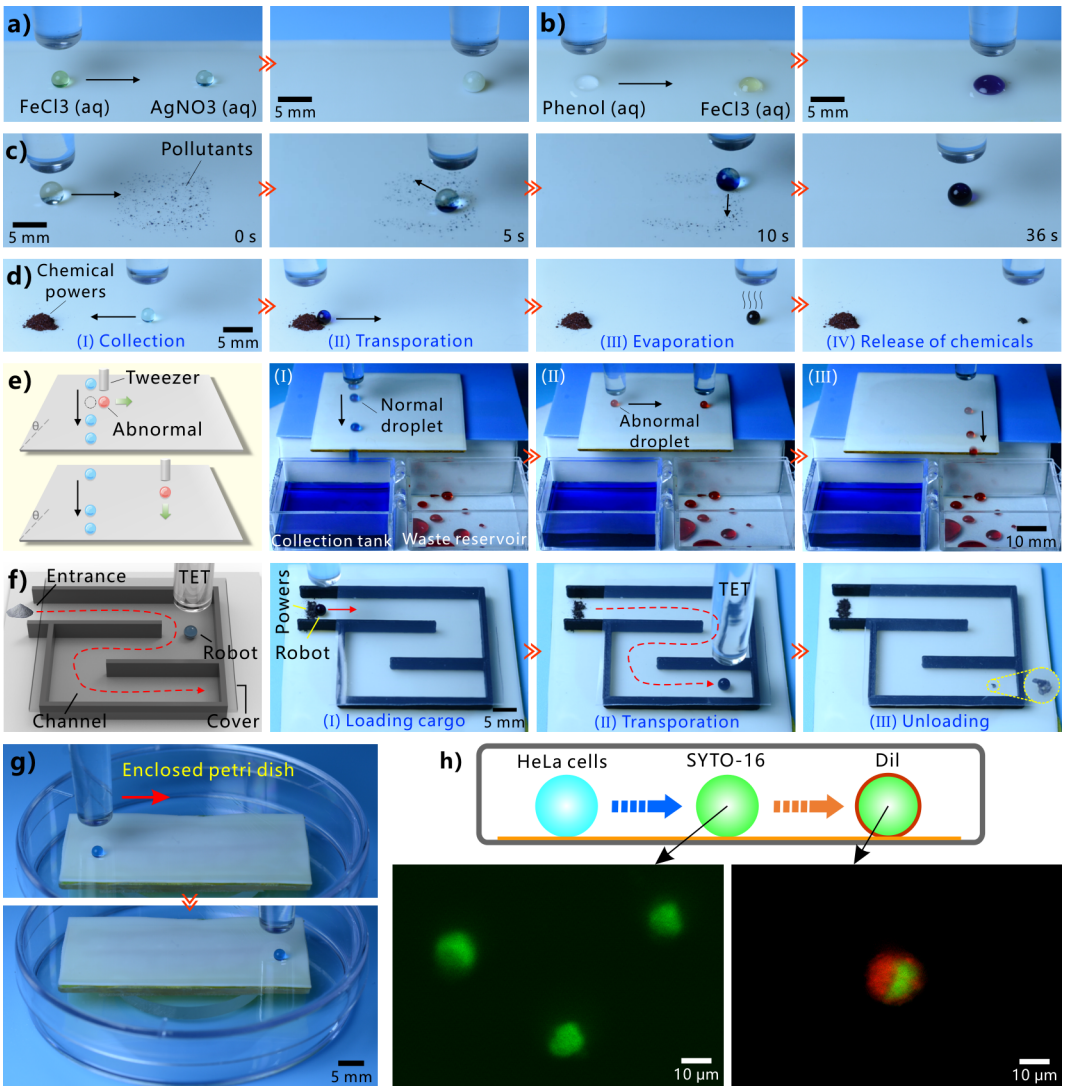

Figure 5. Various applications based on TET droplet manipulation. (a, b) Droplet-based microreaction: (a) inorganic chemical reaction on a superhydrophobic platform and (b) organic chemical reaction on a slippery platform. (c) Controllable and accurate self-cleaning process. (d) Transport and targeted delivery of chemicals (methyl blue powder). (e) Liquid sorting by using TET to remove abnormal droplets from the normal droplet sequence. (f) Soft droplet robot for transporting chemical reagents into a complex closed system. (g) Manipulating a droplet in a closed Petri dish from the outside. (h) Cell labeling in a closed Petri dish: the droplet containing HeLa cells was remotely transported to fuse with an SYTO-16 droplet and further to contact a Dil droplet, which labeled the cell nucleus and membrane, respectively.

where β is the angle from the horizontal plane to the electrostatic force. Because the superhydrophobic platform has extremely low adhesion to droplets, the F_e is easily greater than the adhesion resistance as long as the height of the TET is low and the applied electrostatic potential is large enough. At this time ($F > 0$), the droplets are attracted by electrostatic forces and rapidly move directly below the TET. Moving the TET horizontally will cause the droplet to deviate from the TET, and the droplet will always move toward the spot directly below the TET, so the droplet follows the TET (Figure 1b).

TETs have characteristics of high control precision, strong binding strength, and high flexibility in manipulating droplets. The strong binding strength enables the TET to drive droplets upward along the inclined surface against gravity (Figure 4a and Movie S5) and manipulate large flat-shaped droplets up to 1 mL (Figure 4b and Movie S5). In addition, multiple droplets can be moved simultaneously and in parallel by a single charged rod (Figure 4c and Movie S5). The accumulation of the same charge at the top of each droplet causes the droplets to repel each other, so the droplets do not merge and can move together with a single TET (Figure S3). Of course, we can also use multiple TETs to operate multiple droplets at the same time, with each TET operating one droplet independently, as long as the distance between the TETs is not too small to avoid mutual interference (Figure S4).

PTFE substrates have an excellent chemical inertness. The stability of the superhydrophobic platform allows the TET to transport various corrosive and ionic liquids, such as acid HCl droplets (pH = 2), alkali NaOH droplets (pH = 12), and 10% NaCl salt droplets (Figure 4d and Movie S6). Even if the structured PTFE surface is heated at 200 °C for 12 h, it still maintains excellent superhydrophobicity and supports normal droplet manipulation (Figure 4e and Movie S6).

TETs are also suitable for electrically conductive platforms. For example, droplets on superhydrophobic stainless steel (Figure S6) can be easily moved forward by TET (Figure 4f and Movie S7). *Nepenthes*-inspired lubricant-infused slippery surfaces also exhibit remarkable liquid repellence and extremely

https://doi.org/10.1021/acs.nanolett.4c01953
Nano Lett. 2024, 24, 7116−7124

low adhesion to droplets.[42,43] When a slippery surface is used as a platform, even low-surface-tension ethanol droplets can be moved by a TET (Figure 4g and Movie S7). In particular, an electrostatic field can penetrate insulating materials, allowing TETs to manipulate droplets in a confined space from the outside, such as in a polystyrene (PS) plastic tube (Figure 4h and Movie S8). In some special applications where enclosed spaces cannot be opened (or are not allowed to open) or where the operating tools cannot reach the inside of the closed system, this type of outside-controlling-inner technology is urgently needed. As depicted in Figure 4i, our TET demonstrates overwhelmingly collective performance over other representative droplet manipulation methods in terms of droplet motion behavior, manipulation conditions, and fewer restrictions on the droplet itself (see Supplementary Note S4).[19,24,26,44−46]

The high-precision operation allows the TET to move droplets precisely to the target position. Tiny chemical reactions based on droplets, also known as droplet microreactions, can be achieved by the TET droplet manipulation. As shown in Figure 5a and Movie S9, when a $FeCl_3$ droplet was moved to contact another $AgNO_3$ droplet, a white precipitate formed ($Cl^- + Ag^+ \rightarrow AgCl\downarrow$). In addition to inorganic reactions, even organic microreactions can be achieved on a slippery surface (Figure 5b and Movie S9). The high flexibility of the TET allows the droplet to move along any designed trajectory. In self-cleaning applications, the droplets can be moved to accurately locate contaminants and remove them from the superhydrophobic surface (Figure 5c and Movie S10).[47,48] The droplets can be used as wheels to carry the goods. Figure S6 and Movie S11 show a droplet carrying a small plastic ball. By controlling the movement of the droplet, the plastic ball is moved. This transport process also enables the targeted delivery of chemicals (Figure 5d and Movie S12). A droplet was first moved to a chemical storage place, allowing the chemical (e.g., powder) to dissolve into the droplet. The droplet was then moved to the target location by the TET. Finally, the carried chemical substances were released at the destination after the droplet was completely evaporated, realizing a fixed-point delivery of chemicals. As shown in Figure 5e and Movie S13, the TET can be used for liquid sorting by removing abnormal droplets (red) from the normal droplet sequence (blue). The deformability and flexibility of the droplet allow it to be used as a soft robot. TETs can guide droplet robots through difficult tasks in small or complex spaces, such as delivering chemicals into the interior of a complex closed system with multiple turns (Figure 5f and Movie S14). It is difficult for traditional operating tools to reach inside the confined structure, but the TET can move the droplet robot inside the system from outside the system.

Some special applications require remote manipulation of liquids in a closed system. TETs have the ability to perform contactless droplet operation from the outside of a closed system. Figure 5g and Movie S15 show the process of moving a water droplet in a closed PS Petri dish from the outside. Furthermore, TET droplet manipulation can finish a basic cell labeling experiment in this enclosed Petri dish, as shown in Figure 5h. A droplet containing HeLa cells was transported by TET to fuse with a PBS aqueous droplet containing a 2 μL/mL SYTO-16 stain from the outside of the closed dish. The cell nucleus was stained. The merged droplet was further moved to contact a droplet containing 5 μM Dil to label the cell membrane. Without opening the culture system, the cell nucleus and cell membrane were fluorescently labeled green and red, respectively. During the entire labeling process, the closed nature of the system effectively prevents the cells from being polluted by the external environment and ensures the stability of the gas environment for cell culture.

In conclusion, we developed a portable TET that can manipulate droplets freely on a superhydrophobic platform by induced electrostatic forces. TET droplet manipulation is characterized by high precision, high flexibility, and strong binding strength to droplets. More notably, the TET can also be directly held to manipulate the droplet, demonstrating superior portability. The TET can drive the droplets' flexibly in any direction, without the limitation of the traveling distance. The operating speed can even reach 101.8 mm/s. These advanced capabilities enable the TET to achieve a wide variety of fluid applications, such as droplet-based microreactions, controllable and precise self-cleaning, solid cargo transportation, targeted chemical delivery, liquid sorting, soft droplet robotics, and cell labeling. In particular, TET was demonstrated to be able to manipulate droplets in a closed system from the outside, such as performing cell labeling without opening the culture system.

■ ASSOCIATED CONTENT

Supporting Information

The Supporting Information is available free of charge at https://pubs.acs.org/doi/10.1021/acs.nanolett.4c01953.

Experimental section; detailed description of multifunctional droplet manipulation; detailed description of various droplet manipulation applications; detailed comparison of the TET with other reported droplet manipulation methods; rolling process of a droplet on the superhydrophobic PTFE surface; change in the position and velocity of a droplet in the clawing back process; schematic diagram of the parallel manipulation of multiple droplets by a single charged rod; effect of the distance between two TETs on droplet manipulation; superhydrophobicity of the stainless steel surface; transporting a plastic ball by using a droplet as the wheel; schematic diagram of measuring and adjusting the electrostatic potential of the charged rod (PDF)

Movie S1. Process of TET clawing back a droplet that deviates from its center (MP4)

Movie S2. Round-trip process of manipulating a droplet by TET (MP4)

Movie S3. TET guiding a droplet through a complex maze (MP4)

Movie S4. Shape variation of the droplet as the height of the charged rod gradually decreases (MP4)

Movie S5. Manipulation of a droplet upward along an inclined surface, a large droplet with a volume of 1 mL, and parallel multiple droplets (MP4)

Movie S6. Manipulation of various corrosive droplets (including acid, alkali, and salt solutions) and the droplets on the surface after heating treatment (MP4)

Movie S7. Manipulation of a water droplet on an electrically conductive superhydrophobic stainless steel surface and an ethanol droplet on a lubricated slippery PTFE surface (MP4)

Movie S8. Manipulating a droplet in an enclosed plastic tube from the outside (MP4)

Movie S9. Droplet-based microreactions (MP4)

Movie S10. Controllable and accurate self-cleaning process (MP4)

https://doi.org/10.1021/acs.nanolett.4c01953
Nano Lett. 2024, 24, 7116−7124

Movie S11. Transporting a plastic ball by using a droplet as the wheel (MP4)
Movie S12. Transport and targeted delivery of chemicals (MP4)
Movie S13. Liquid sorting by removing abnormal droplets from the normal droplet sequence (MP4)
Movie S14. Soft droplet robot for transporting chemical reagents into a complex closed system (MP4)
Movie S15. Manipulating a droplet in a closed Petri dish from the outside (MP4)

AUTHOR INFORMATION

Corresponding Authors

Chaowei Wang − *CAS Key Laboratory of Mechanical Behavior and Design of Materials, Department of Precision Machinery and Precision Instrumentation, University of Science and Technology of China, Hefei 230027, People's Republic of China*; Email: chaoweiw@ustc.edu.cn

Dong Wu − *CAS Key Laboratory of Mechanical Behavior and Design of Materials, Department of Precision Machinery and Precision Instrumentation, University of Science and Technology of China, Hefei 230027, People's Republic of China*; orcid.org/0000-0003-0623-1515; Email: dongwu@ustc.edu.cn

Authors

Jiale Yong − *CAS Key Laboratory of Mechanical Behavior and Design of Materials, Department of Precision Machinery and Precision Instrumentation, University of Science and Technology of China, Hefei 230027, People's Republic of China*

Xinlei Li − *CAS Key Laboratory of Mechanical Behavior and Design of Materials, Department of Precision Machinery and Precision Instrumentation, University of Science and Technology of China, Hefei 230027, People's Republic of China*

Youdi Hu − *CAS Key Laboratory of Mechanical Behavior and Design of Materials, Department of Precision Machinery and Precision Instrumentation, University of Science and Technology of China, Hefei 230027, People's Republic of China*

Yiming Wang − *CAS Key Laboratory of Mechanical Behavior and Design of Materials, Department of Precision Machinery and Precision Instrumentation, University of Science and Technology of China, Hefei 230027, People's Republic of China*

Yubin Peng − *CAS Key Laboratory of Mechanical Behavior and Design of Materials, Department of Precision Machinery and Precision Instrumentation, University of Science and Technology of China, Hefei 230027, People's Republic of China*; orcid.org/0000-0002-2917-6830

Zhenrui Chen − *CAS Key Laboratory of Mechanical Behavior and Design of Materials, Department of Precision Machinery and Precision Instrumentation, University of Science and Technology of China, Hefei 230027, People's Republic of China*

Yachao Zhang − *CAS Key Laboratory of Mechanical Behavior and Design of Materials, Department of Precision Machinery and Precision Instrumentation, University of Science and Technology of China, Hefei 230027, People's Republic of China*; orcid.org/0000-0002-4468-6142

Suwan Zhu − *CAS Key Laboratory of Mechanical Behavior and Design of Materials, Department of Precision Machinery and Precision Instrumentation, University of Science and Technology of China, Hefei 230027, People's Republic of China*; orcid.org/0000-0001-9881-5694

Complete contact information is available at: https://pubs.acs.org/10.1021/acs.nanolett.4c01953

Notes

The authors declare no competing financial interest.

ACKNOWLEDGMENTS

This work was supported by the USTC Research Funds of the Double First-Class Initiative (No. YD2090002013) and the National Natural Science Foundation of China (Nos. 61927814, 62325507, 52122511, and U20A20290). We acknowledge the Experimental Center of Engineering and Material Sciences at USTC for the fabrication and measurement of the samples. This work was partly carried out at the USTC Center for Micro- and Nanoscale Research and Fabrication.

REFERENCES

(1) Abdelgawad, M.; Wheeler, A. R. The Digital Revolution: A New Paradigm for Microfluidics. *Adv. Mater.* **2009**, *21*, 920−925.
(2) Seemann, R.; Brinkmann, M.; Pfohl, T.; Herminghaus, S. Droplet based Microfluidics. *Rep. Prog. Phys.* **2012**, *75*, 016601.
(3) Jokinen, V.; Sainiemi, L.; Franssila, S. Complex Droplets on Chemically Modified Silicon Nanograss. *Adv. Mater.* **2008**, *20*, 3453−3456.
(4) Dong, Z.; Ma, J.; Jiang, L. Manipulating and Dispensing Micro/Nanoliter Droplets by Superhydrophobic Needle Nozzles. *ACS Nano* **2013**, *7*, 10371−10379.
(5) Song, J.; Cheng, W.; Nie, M.; He, X.; Nam, W.; Cheng, J.; Zhou, W. Partial Leidenfrost Evaporation-Assisted Ultrasensitive Surface-Enhanced Raman Spectroscopy in a Janus Water Droplet on Hierarchical Plasmonic Micro-/Nanostructures. *ACS Nano* **2020**, *14*, 9521−9531.
(6) Hajji, I.; Serra, M.; Geremie, L.; Ferrante, I.; Renault, R.; Viovy, J.-L.; Descroix, S.; Ferraro, D. Droplet Microfluidic Platform for Fast and Continuous-Flow RT-qPCR Analysis Devoted to Cancer Diagnosis Application. *Sens. Actuators B Chem.* **2020**, *303*, 127171.
(7) Wu, D.; Zhang, Z.; Zhang, Y.; Jiao, Y.; Jiang, S.; Wu, H.; Li, C.; Zhang, C.; Li, J.; Hu, Y.; Li, G.; Chu, J.; Jiang, L. High-Performance Unidirectional Manipulation of Microdroplet by Horizontal Vibration on Femtosecond Laser-Induced Slant Microwalls Array. *Adv. Mater.* **2020**, *32*, 2005039.
(8) Bai, X.; Yang, Q.; Fang, Y.; Yong, J.; Bai, Y.; Zhang, J.; Hou, X.; Chen, F. Anisotropic, Adhesion-Switchable, and Thermal-Responsive Superhydrophobicity on the Femtosecond laser-Structured Shape-Memory Polymer for Droplet Manipulation. *Chem. Eng. J.* **2020**, *400*, 125930.
(9) Zheng, Y.; Bai, H.; Huang, Z.; Tian, X.; Nie, F.-Q.; Zhao, Y.; Zhai, J.; Jiang, L. Directional Water Collection on Wetted Spider Silk. *Nature* **2010**, *463*, 640−643.
(10) Zhang, S.; Huang, J.; Chen, Z.; Lai, Y. Bioinspired Special Wettability Surfaces: From Fundamental Research to Water Harvesting Applications. *Small* **2017**, *13*, 1602992.
(11) Jiang, M.; Wang, Y.; Liu, F.; Du, H.; Li, Y.; Zhang, H.; To, S.; Wang, S.; Pan, C.; Yu, J.; Quéré, D.; Wang, Z. Inhibiting the Leidenfrost Effect above 1000 °C for Sustained Thermal Cooling. *Nature* **2022**, *601*, 568−572.
(12) Cheng, Z.; Wang, C.; Li, X.; Xu, T.; Chen, Z.; Cui, Z.; Cheng, K.; Zhu, S.; Wu, D.; Yong, J. Designable and Unidirectional Motion of Leidenfrost Droplets on Heated Asymmetric Microgrooves Written by Femtosecond Laser. *Appl. Phys. Lett.* **2024**, *124*, 061601.
(13) Xu, J.; Xiu, S.; Lian, Z.; Yu, H.; Cao, J. Bioinspired Materials for Droplet Manipulation: Principles, Methods and Applications. *Droplet* **2022**, *1*, 11−37.

(14) Lin, F.; Wo, K.; Fan, X.; Wang, W.; Zou, J. Directional Transport of Underwater Bubbles on Solid Substrates: Principles and Applications. *ACS Appl. Mater. Interfaces* **2023**, *15*, 10325−10340.
(15) Lv, P.; Zhang, Y.-L.; Han, D.-D.; Sun, H.-B. Directional Droplet Transport on Functional Surfaces with Superwettabilities. *Adv. Mater. Interfaces* **2021**, *8*, 2100043.
(16) Hernandez, S. C.; Bennett, C. J.; Junkermeier, C. E.; Tsoi, S. D.; Bezares, F. J.; Stine, R.; Robinson, J. T.; Lock, E. H.; Boris, D. R.; Pate, B. D.; Caldwell, J. D.; Reinecke, T. L.; Sheehan, P. E.; Walton, S. G. Chemical Gradients on Graphene to Drive Droplet Motion. *ACS Nano* **2013**, *7*, 4746−4755.
(17) Yu, C.; Cao, M.; Dong, Z.; Wang, J.; Li, K.; Jiang, L. Spontaneous and Directional Transportation of Gas Bubbles on Superhydrophobic Cones. *Adv. Funct. Mater.* **2016**, *26*, 3236−3243.
(18) Xiao, X.; Zhang, C.; Ma, H.; Zhang, Y.; Liu, G.; Cao, M.; Yu, C.; Jiang, L. Bioinspired Slippery Cone for Controllable Manipulation of Gas Bubbles in Low-Surface-Tension Environment. *ACS Nano* **2019**, *13*, 4083−4090.
(19) Sun, Q.; Wang, D.; Li, Y.; Zhang, J.; Ye, S.; Cui, J.; Chen, L.; Wang, Z.; Butt, H.-J.; Vollmer, D.; Deng, X. Surface Charge Printing for Programmed Droplet Transport. *Nat. Mater.* **2019**, *18*, 936−941.
(20) Han, X.; Jin, R.; Sun, Y.; Han, K.; Che, P.; Wang, X.; Guo, P.; Tan, S.; Sun, X.; Dai, H.; Dong, Z.; Heng, L.; Jiang, L. Infinite Self-Propulsion of Circularly On/Discharged Droplets. *Adv. Mater.* **2024**, *36*, 2311729.
(21) Yong, J.; Peng, Y.; Wang, X.; Li, J.; Hu, Y.; Chu, J.; Wu, D. Self-Driving Underwater "Aerofluidics. *Adv. Sci.* **2023**, *10*, 2301175.
(22) Jiang, S.; Wu, D.; Li, J.; Chu, J.; Hu, Y. Magnetically Responsive Manipulation of Droplets and Bubbles. *Droplet* **2024**, *3*, No. e117.
(23) Wang, F.; Liu, M.; Liu, C.; Wang, T.; Wang, Z.; Du, X. Light-Induced Charged Slippery Surfaces. *Sci. Adv.* **2022**, *8*, No. eabp9369.
(24) Li, W.; Tang, X.; Wang, L. Photopyroelectric Microfluidics. *Sci. Adv.* **2020**, *6*, No. eabc1693.
(25) Jin, Y.; Wu, C.; Sun, P.; Wang, M.; Cui, M.; Zhang, C.; Wang, Z. Electrification of Water: From Basics to Applications. *Droplet* **2022**, *1*, 92−109.
(26) Jin, Y.; Xu, W.; Zhang, H.; Li, R.; Sun, J.; Yang, S.; Liu, M.; Mao, H.; Wang, Z. Electrostatic Tweezer for Droplet Manipulation. *Proc. Natl. Acad. Sci. U.S.A.* **2022**, *119*, No. e2105459119.
(27) Yong, J.; Li, X.; Hu, Y.; Peng, Y.; Cheng, Z.; Xu, T.; Wang, C.; Wu, D. Triboelectric "Electrostatic Tweezers" for Manipulating Droplets on Lubricated Slippery Surfaces Prepared by Femtosecond Laser Processing. *Int. J. Extrem. Manuf.* **2024**, *6*, 035002.
(28) Yuan, Z.; Lu, C.; Liu, C.; Bai, X.; Zhao, L.; Feng, S.; Liu, Y. Ultrasonic Tweezer for Multifunctional Droplet Manipulation. *Sci. Adv.* **2023**, *9*, No. eadg2352.
(29) Demirör, A. F.; Aykut, S.; Ganzeboom, S.; Meier, Y. A.; Poloni, E. Programmable Droplet Manipulation and Wetting with Soft Magnetic Carpets. *Proc. Natl. Acad. Sci. U.S.A.* **2021**, *118*, No. e2111291118.
(30) Ren, S.; Ning, Y.; Zhao, Z.; Li, Q.; Zhang, X.; Jiang, L.; Liu, K. Underwater Directional and Continuous Manipulation of Gas Bubbles on Superaerophobic Magnetically Responsive Microcilia Array. *Adv. Funct. Mater.* **2022**, *32*, 2112274.
(31) Zhu, S.; Bian, Y.; Wu, T.; Chen, C.; Jiao, Y.; Jiang, Z.; Huang, Z.; Li, E.; Li, J.; Chu, J.; Hu, Y.; Wu, D.; Jiang, L. High Performance Bubble Manipulation on Ferrofluid-Infused Laser-Ablated Microstructured Surfaces. *Nano Lett.* **2020**, *20*, 5513−5521.
(32) Ristenpart, W. D.; Bird, J. C.; Belmonte, A.; Dollar, F.; Stone, H. A. Non-Coalescence of Oppositely Charged Drops. *Nature* **2009**, *461*, 377−380.
(33) Han, X.; Tan, S.; Jin, R.; Jiang, L.; Heng, L. Noncontact Charge Shielding Knife for Liquid Microfluidics. *J. Am. Chem. Soc.* **2023**, *145*, 6420−6427.
(34) Chang, J.-S.; Lawless, P. A.; Yamamoto, T. Corona Discharge Processes. *IEEE Transactions on Plasma Science* **1991**, *19*, 1152−1166.
(35) Tang, Q.; Liu, X.; Cui, X.; Su, Z.; Zheng, H.; Tang, J.; Joo, S. W. Contactless Discharge-Driven Droplet Motion on a Nonslippery Polymer Surface. *Langmuir* **2021**, *37*, 14697−14702.
(36) Han, K.; Wang, Z.; Han, X.; Wang, X.; Guo, P.; Che, P.; Heng, L.; Jiang, L. Active Manipulation of Functional Droplets on Slippery Surface. *Adv. Funct. Mater.* **2022**, *32*, 2207738.
(37) Link, D. R.; Grasland-Mongrain, E.; Duri, A.; Sarrazin, F.; Cheng, Z.; Cristobal, G.; Marquez, M.; Weitz, D. A. Electric Control of Droplets in Microfluidic Devices. *Angew. Chem., Int. Ed.* **2006**, *45*, 2556−2560.
(38) Wang, F.; Guo, F.; Wang, Z.; He, H.; Sun, Y.; Liang, W.; Yang, B. Surface Charge Density Gradient Printing To Drive Droplet Transport: A Numerical Study. *Langmuir* **2022**, *38*, 13697−13706.
(39) Han, X.; Tan, S.; Wang, Q.; Zuo, X.; Heng, L.; Jiang, L. Noncontact Microfluidics of Highly Viscous Liquids for Accurate Self-Splitting and Pipetting. *Adv. Mater.* **2024**, *36*, 2402779.
(40) Xu, W.; Jin, Y.; Li, W.; Song, Y.; Guo, S.; Zhang, B.; Wang, L.; Cui, M.; Yan, X.; Wang, Z. Triboelectric Wetting for Continuous Droplet Transport. *Sci. Adv.* **2022**, *8*, No. eade2085.
(41) Jin, Y.; Liu, X.; Xu, W.; Sun, P.; Huang, S.; Yang, S.; Yang, X.; Wang, Q.; Lam, R. H. W.; Li, R.; Wang, Z. Charge-Powered Electrotaxis for Versatile Droplet Manipulation. *ACS Nano* **2023**, *17*, 10713−10720.
(42) Wong, T. S.; Kang, S. H.; Tang, S. K.; Smythe, E. J.; Hatton, B. D.; Grinthal, A.; Aizenberg, J. Bioinspired Self-Repairing Slippery Surfaces with Pressure-Stable Omniphobicity. *Nature* **2011**, *477*, 443−447.
(43) Yong, J.; Huo, J.; Yang, Q.; Chen, F.; Fang, Y.; Wu, X.; Liu, L.; Lu, X.; Zhang, J.; Hou, X. Femtosecond Laser Direct Writing of Porous Network Microstructures for Fabricating Super-Slippery Surfaces with Excellent Liquid Repellence and Anti-Cell Proliferation. *Adv. Mater. Interfaces* **2018**, *5*, 1701479.
(44) Zhang, X.; Ben, S.; Zhao, Z.; Ning, Y.; Li, Q.; Long, Z.; Yu, C.; Liu, K.; Jiang, L. Lossless and Directional Transport of Droplets on Multi-Bioinspired Superwetting V-Shaped Rails. *Adv. Funct. Mater.* **2023**, *33*, 2212217.
(45) Wang, L.; Zhang, C.; Wei, Z.; Xin, Z. Bioinspired Fluoride-Free Magnetic Microcilia Arrays for Anti-Icing and Multidimensional Droplet Manipulation. *ACS Nano* **2024**, *18*, 526−538.
(46) Li, A.; Li, H.; Li, Z.; Zhao, Z.; Li, K.; Li, M.; Song, Y. Programmable Droplet Manipulation by a Magnetic-Actuated Robot. *Sci. Adv.* **2020**, *6*, No. eaay5808.
(47) Nishimoto, S.; Bhushan, B. Bioinspired Self-Cleaning Surfaces with Superhydrophobicity, Superoleophobicity, and Superhydrophilicity. *RSC Adv.* **2013**, *3*, 671−690.
(48) Yong, J.; Yang, Q.; Chen, F.; Zhang, D.; Bian, H.; Ou, Y.; Si, J.; Du, G.; Hou, X. Stable Superhydrophobic Surface with Hierarchical Mesh-Porous Structure Fabricated by a Femtosecond Laser. *Appl. Phys. A: Mater. Sci. Process.* **2013**, *111*, 243−249.

https://doi.org/10.1021/acs.nanolett.4c01953
Nano Lett. 2024, 24, 7116−7124